

NUMERICAL SIMULATION OF CHLORIDE DIFFUSION IN REINFORCED CONCRETE STRUCTURES WITH CRACKS

CHRISTOPHER K Y LEUNG* DONGWEI HOU*

* Department of Civil and Environmental Engineering
The Hong Kong University of Science and Technology (HKUST)
Clear Water Bay, Kowloon, Hong Kong
e-mail: houdw@ust.hk, www.ust.hk

Key words: Chloride diffusion; effect of cracking; equivalent diffusion coefficient; durability

Abstract: Steel corrosion is a major problem with concrete structures. For concrete structures exposed to chlorides, once a critical chloride concentration is reached at the steel surface, corrosion starts to occur. For a given cover thickness, the corrosion initiation time depends on the chloride diffusivity. The diffusivity D_0 for concrete is normally measured at the un-cracked state. However, in reinforced concrete design, concrete members are allowed to crack in tension. Once cracking occurs, chloride can also diffuse through the crack at a faster rate governed by the crack diffusivity D_{cr} . In the present study, finite element analysis is performed to study the effect of cracking on corrosion initiation in concrete with different values of D_0 . For various crack width and cover thickness, the time for critical chloride concentration to be reached at steel intersected by the crack is determined. Based on the simulation results, we derive the empirical equation for an equivalent diffusion coefficient (D_{eq}) which can be employed directly in the solution of the one-dimensional diffusion equation to calculate the corrosion initiation time. The study provides a convenient but accurate approach for predicting corrosion initiation under real world situations where cracks are present in a concrete structure.

1 INTRODUCTION

Steel corrosion is a major problem with concrete structures. In the alkaline environment inside concrete, steel is in the passivated state with a thin surface layer of stable iron oxide to protect it from corrosion. For concrete structures exposed to chlorides, the chloride concentration at the surface of steel

reinforcements will increase with time due to the diffusion process. Once a critical chloride concentration is reached, the steel is depassivated and corrosion starts to occur. For a given cover thickness, the corrosion initiation time depends on the chloride diffusivity of the concrete. Many researchers have measured the diffusivity of concrete at its virgin state [1-3].

However, in reinforced concrete design, concrete members are allowed to crack in tension. The effect of cracks on chloride diffusivity is therefore an important issue to be studied.

In Aldea et al. [4], the Rapid Chloride Penetration Test (RCPT) was performed on loaded concrete discs with discrete tensile cracks from 0.05mm to 0.4mm in width. For normal strength concrete samples, chloride permeability was found to be much less sensitive to crack opening than high strength concrete with lower permeability in the un-cracked state. In Gerard and Marchand [5], the coefficient of chloride diffusivity (D_{Cl}) was measured for specimens cracked under freezing/thawing with the two cell migration test, in which a concrete disc is placed between two cells with solutions of different chloride concentration. Results indicated that D_{Cl} would increase with the number and opening of cracks. Olga and Hooton [6] performed bulk chloride diffusion test on concrete specimens containing artificial cracks with openings between 0.10 mm to 0.68 mm. In the test, one face of the specimens was exposed to chlorides, and D_{Cl} was determined from the chloride profile in the specimen. According to the test results, the value of D_{Cl} is not dependent on crack opening within the tested range. However, since the cracks in the samples are artificial ones introduced in a certain special way, the findings may not apply quantitatively to concrete with cracks formed under loading.

To date, the most comprehensive study on the effect of cracks on chloride diffusivity was conducted by Djerbi et al [7]. In this work, concrete discs made with three different kinds of concrete were subjected to split tension to produce discrete cracks of various openings. The cracked discs (as well as control specimens with no cracks) were tested in the chloride migration cell with both chloride concentration gradient and electric potential across the two

sides of the sample. The value of D_{Cl} for each specimen was obtained from the change of chloride concentration in the downstream cell after steady state had been reached. Based on a parallel flow model first proposed by Gerard and Marchand [5] for the steady state, the chloride diffusivity of the crack (D_{cr}) was determined and plotted against the crack width. Interestingly, D_{cr} was found to be dependent on crack width but not the diffusivity of un-cracked concrete (D_o). This explains the observation in Aldea et al [4] that a crack has larger effect on concrete with lower diffusivity, as D_{cr} is much higher than D_o for such a case.

Knowing the value of D_{cr} for a particular crack width, analysis of the chloride diffusion process in cracked concrete can take into consideration the increased diffusivity along the crack. In this study, the finite element method is employed to study the effect of crack width on corrosion initiation in concrete with various values of D_o . In the analysis, adjacent cracks are assumed to be sufficiently far away from one another so we can neglect interactive effects and focus on a single crack. Based on the simulation results, an empirical equation will be derived for the equivalent diffusion coefficient (D_{eq}) which can be used directly for calculating the corrosion initiation time in cracked concrete.

2 NUMERICAL SIMULATION

2.1 Outline of the simulation approach

For concrete structures exposed to the chloride environment, chloride diffusion through the cover layer can often be considered as a 2-D diffusion process, Fig.1 illustrates the typical situation of a cracked concrete member with one of its surfaces exposed to chloride. If the crack is not present, and the chloride concentration is constant along the surface of the member (in the y-direction), 1-D diffusion occurs in the x-direction. An analytical solution

for the chloride concentration at any point within the concrete can then be obtained. For concrete structures containing cracks, the rate of chloride diffusion through cracks is much higher than that through concrete matrix. The resulted concentration gradient between the crack and adjacent concrete will induce lateral diffusion of chloride along the y-direction as well. The diffusion problem then becomes 2-D in nature. Under such a situation, an analytical solution is very difficult to derive so the finite element method is employed to determine the chloride concentration within the member at various times. The time for critical chloride concentration to be reached at a given concrete cover can then be obtained.

In this study, adjacent cracks in the concrete structure are assumed to be sufficiently far away from one another, so there is no interactive effect among the cracks. It is then only necessary to consider a single crack in the finite element model. To simulate the diffusion process, the ANSYS10.0 FEA software is employed.

Fig. 2 shows a typical finite element mesh of the diffusion domain. The dimension of the model is 200 mm (along the surface) times 200 mm (along the direction of the crack). The focus of the work is to determine the chloride concentration along the crack, because steel corrosion will occur first at the section intersected by the crack. The chosen length of the model is 200 mm, which is significantly higher than the typical steel cover of 30 to 100 mm. When critical chloride concentration is reached at the steel, the chloride concentration at the lower boundary is found (in the simulation results) to be very small so the boundary has little effect on the diffusion process. Similarly, with the width of 100mm, the calculated chloride concentrations at the vertical boundaries were found to be much lower than that along the crack (at the same

value of x), indicating that the boundaries in the model are sufficiently far away from the crack.

To obtain accurate numerical results, the mesh size of concrete matrix is kept within 1 mm, while the mesh size of the crack is refined to less than 0.05 mm. The transition from small to large elements is shown in Fig. 2. The maximum permitted time step is taken to be $\text{ITS} = \delta^2 / 4D$, where δ is the mesh size at the point with highest concentration gradient (along the upper boundary in this case), and D is the corresponding diffusion coefficient.

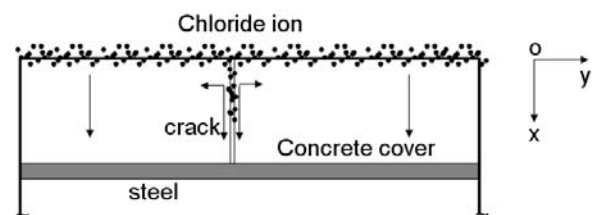


Fig. 1. Diagram of chloride diffusion in cracked concrete

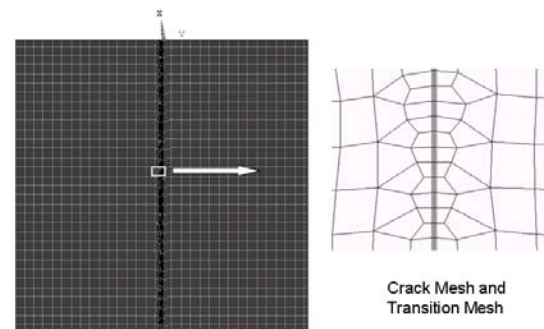


Fig. 2 Mesh of matrix and crack in FEM

While the range of D_0 for concrete is well documented, D_{cr} is dependent on the crack width (w). Based on experimental measurements, Djerbi et al [7] proposed empirical equations to relate D_{cr} to w . When w increases from 30 to 80 μm , D_{cr} increases from 2×10^{-10} to $12 \times 10^{-10} \text{ m}^2/\text{s}$. For larger values of w , D_{cr} remains constant at $12 \times 10^{-10} \text{ m}^2/\text{s}$. In the finite element simulation, instead of following this relation directly, the value of D_{cr} for a given w is allowed to vary within a certain

range. This is to accommodate the possibility of different D_{cr} vs w relation that may be revealed from future experiments. Specifically, D_{cr} varies from 1×10^{-10} to 20×10^{-10} m^2/s . Also, D_o is taken to range from 0.2×10^{-12} m^2/s to 10×10^{-12} m^2/s while w ranges from $30 \mu m$ to $1000 \mu m$. Simulations with various combinations of parameters D_{cr} , D_o and w are performed to cover the whole range. For convenience, the chloride concentration on the member surface is fixed at $C_o = 1000$ g/m^3 . The actual value of C_o is not important as it is the C/C_o ratio which is of interest. The calculated diffusion time is up to 10 years.

2.2 Simulation results

Typical simulation results are shown in Fig.3 for $w = 60 \mu m$ and diffusion time of one year. D_{cr} is taken to be 8×10^{-10} m^2/s . In the simulation, we are comparing the real situation (i.e., a domain with a crack) to two limiting cases: case I with diffusion through un-cracked concrete with $D = D_o = 0.5 \times 10^{-12}$ m^2/s and case II with 1-D diffusion through the crack alone, with $D = D_{cr} = 8 \times 10^{-10}$ m^2/s . Fig.3(a) shows the chloride concentration for the three cases: Case I on the left, the actual situation for cracked concrete in the middle and Case II on the right. It is obvious that the diffusion process is fastest when chloride is assumed to diffuse through the crack alone, with no lateral flow. In reality, however, due to the concentration gradient in the y -direction, chloride penetration in the x -direction can be significantly slowed down, as observed from the results for cracked concrete and Case II. Also, according to the result for cracked concrete, the crack has little influence on diffusion at locations far away from the crack. At such locations, the diffusion process can be considered as 1-D and governed by the surface concentration alone.

Fig. 3(b) shows the variation of normalized chloride concentration with distance from surface (x) for Case I (un-cracked) and variation

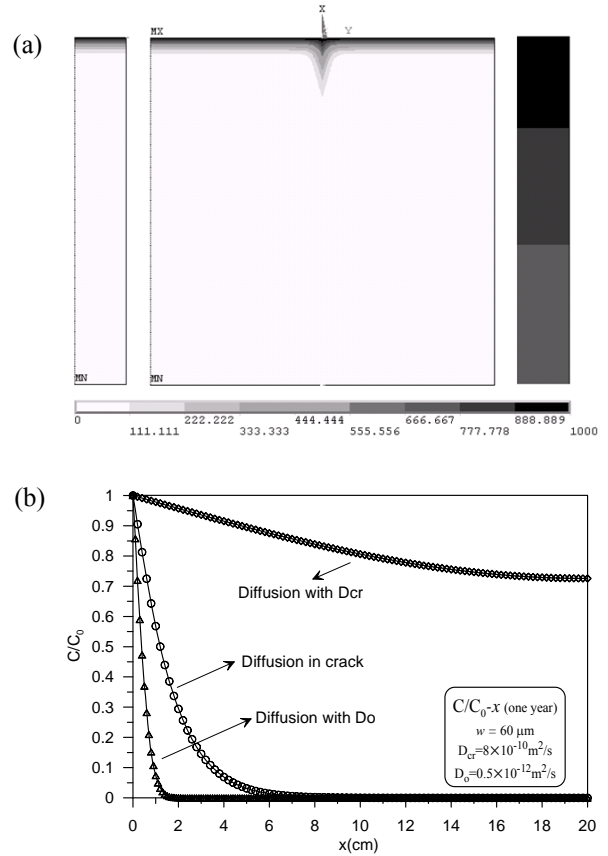


Fig. 3 Chloride diffusion in cracked concrete compared to limiting cases. (a) Plot of chloride concentration, (b) Variation of chloride concentration with distance from surface.

along the crack in Cases II and III. The results again illustrate that it is important to consider the 2-D nature of the diffusion problem. Specifically, if one does not account for the lateral diffusion (i.e., the diffidence effect), chloride penetration is severely over-estimated as indicated by the result for Case II.

Based on physical considerations, one can argue that the diffidence effect decreases with the ratio D_{cr}/D_o , but increases with the ratio A_l/A_w , where A_l is the area for lateral diffusion to occur across the crack surfaces, and A_w is the area for direct diffusion through the crack. A_l/A_w is proportional to the ratio x/w . As w is often very small, x/w can be very large. Therefore, even though D_{cr} is much higher than D_o in many cases, the diffidence effect can still be significant. From this analysis, we can

deduce that the chloride diffusion through crack in high strength concrete will be faster than that in ordinary concrete when the two kinds of concrete have the same width of cracks (i.e. the same D_{cr}), because the high strength concrete owns the lower matrix diffusion coefficient D_o and thus induces the weaker diffuence effect on the chloride diffusion through crack than ordinary strength concrete.

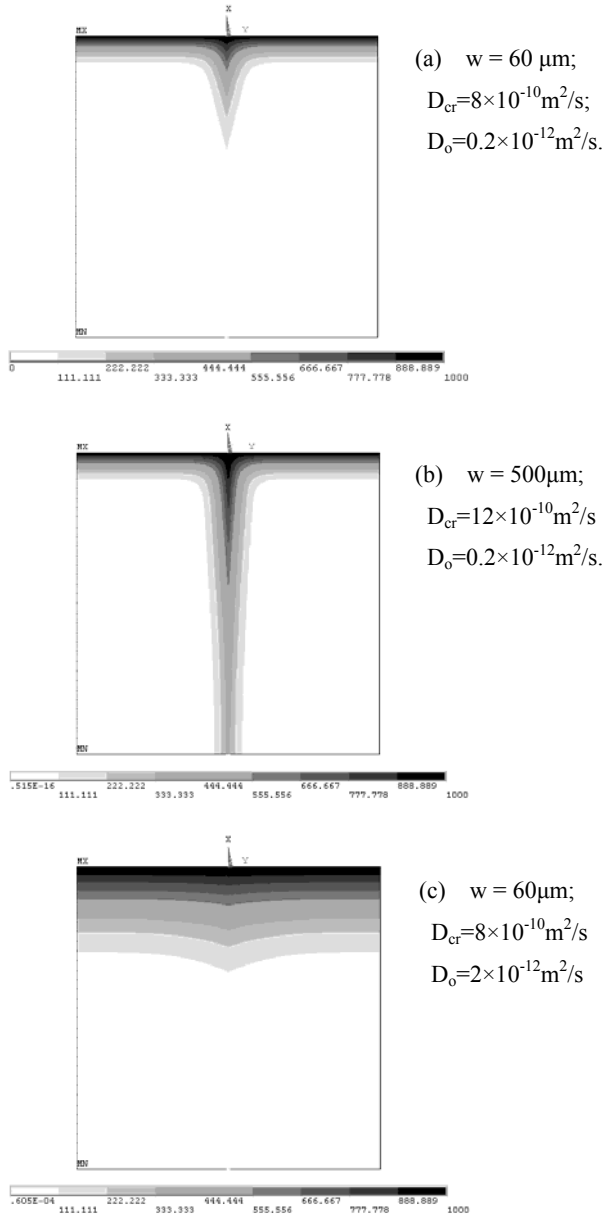


Fig. 4 Typical simulation results of chloride diffusions in cracked concretes

Fig.4 shows three types of chloride distribution in cracked concrete with different combinations of D_{cr} , D_o and w after diffusion has occurred for 5 years. When the D_{cr}/D_o is high and/or w is large, diffusion through the crack will be much faster than that through the concrete matrix, as shown in Fig.4 (a) and Fig.4 (b). When D_{cr}/D_o is low and/or w is small, as in Fig.4(c), the effect of the crack is not too significant.

In practice, we are most interested in the chloride penetration along the crack, as steel corrosion will occur first at the crack's vicinity. To avoid the need to perform computational analysis for every single case, an empirical approach for analyzing chloride diffusion through the crack is proposed. One-dimensional diffusion is assumed to occur and the equivalent diffusion coefficient (D_{eq}) is determined empirically from the fitting of numerical results. With a general expression for D_{eq} , the chloride concentration along the crack under any combination of D_{cr} , D_o , w and time can be obtained, details of the empirical approach are discussed in the following sections.

3 EMPIRICAL MODELING OF DIFFUSION THROUGH CRACK

3.1 Equivalent diffusion coefficient

As mentioned above, diffusion through the crack is affected by the diffuence effect in the y -direction (which is perpendicular to the crack). Based on mass conservation, the chloride concentration (C_{cr}) along the crack can be obtained from the following equation:

$$\frac{\partial C_{cr}}{\partial t} = D_{cr} \frac{\partial^2 C_{cr}}{\partial x^2} + \frac{2D_o}{w} G(x) \quad (1)$$

where $G(x)$ is absolute value of $\partial C/\partial y$ at $y = \pm w/2$ (i.e., the boundaries of the crack), in

unit of g/m^4 . As eqn (1) is very difficult to solve, a semi-empirical approach is proposed to replace it with the equation for 1-D diffusion:

$$\frac{\partial C_{\text{cr}}}{\partial t} = D_{\text{eq}} \frac{\partial^2 C_{\text{cr}}}{\partial x^2} \quad (2)$$

Where

$$D_{\text{eq}} = D_{\text{cr}} + D_0 \frac{2G(x)}{w \cdot \frac{\partial^2 C_{\text{cr}}}{\partial x^2}} \quad (3)$$

For the sake of simplicity, D_{eq} can be further expressed in the following form

$$D_{\text{eq}} = D_{\text{cr}} - K \cdot D_0 \quad (4)$$

Eqn (4) indicates that D_{eq} will be smaller than D_{cr} due to the diffidence effect. It is clear that D_{eq} and K are not constants. Generally speaking, they are functions of various parameters including D_{cr} (m^2/s), D_0 (m^2/s) and w (m), as well as distance from the external boundary x (m) and diffusion age t (s). In Djerbi et al [7], a relation between D_{cr} and w was proposed. However, as mentioned above, different researchers have reported different effects of w on D_{cr} . In the present study, to make the model more general and applicable to data from different investigations (including those to be obtained in the future), D_{cr} and w are treated as two separate variables.

To obtain D_{eq} for a particular combination of D_{cr} , D_0 , w , x and t from the finite element result, the classical solution for one-dimension diffusion is employed:

$$C_{\text{cr}}(x, t) = C_0 \operatorname{erfc} \left(\frac{x}{2\sqrt{D_{\text{eq}}t}} \right) \quad (5)$$

Eqn (5) is not a solution to eqn (2) because D_{eq} is not constant. The use of this equation to obtain D_{eq} is simply for convenience. Once we have carried out a sufficient number of

numerical simulations, an empirical expression for D_{eq} will be determined in terms of the various parameters through data fitting. With this empirical expression, the chloride concentration along the crack can be easily obtained from eqn (5).

3.2 Range of valid numerical data

As in any computational method, results of the finite element model are subject to numerical error. In the fitting of finite element results, it is important to avoid data with high inaccuracy. The two major reasons for inaccurate numerical data are discussed below.

In the derivation of the diffusion equation, the transfer speed of chlorides is assumed to be infinite [8]. As a result, the chloride concentration at any point in the computational domain is non-zero once the diffusion process begins (i.e. $t > 0$). This is clearly revealed from eqn (5), which is the solution for the 1-D diffusion equation. At locations far away from the surface, very small values of chloride concentration will be calculated. For such results, the numerical error will be very high, leading to inaccurate values of D_{eq} in eqn (5). For a given distance from the surface, the calculated concentration can only be considered valid after the diffusion process has gone on for a sufficiently long time. Determination of this 'minimum' time value is best illustrated with the un-cracked case, the results of which are given in Fig.5. Fig.5(a) shows the variation of matrix diffusion coefficient D_0 (calculated from numerical results according to eqn(5)) with distance from surface x . For diffusion ages of 6 months, 1 year, 3 years, 5 years and 10 years, D_0 begins to deviate from the correct value of $0.2 \times 10^{-12} \text{ m}^2/\text{s}$ beyond the distances of 1.1 cm, 1.8 cm, 3.1cm, 4.0 cm, 5.1cm and 5.5 cm respectively.. The increase of D_0 is caused by the significant relative error of the low computed chloride concentration. For a certain diffusion age, the finite element result can only

be considered valid for points within a certain distance from the surface. Beyond the critical distance, notable error arises. Conversely, for a certain distance from the surface, only after a sufficient long time of diffusion is the simulated chloride concentration valid and hence suitable for computing D_o .

To help identify the critical distance for data to be valid, the derivative of D_o ($\partial D_o / \partial x$) is plotted against x for different diffusion times in Fig. 5(b). The derivative is initially zero but begins rising after a certain distance from the surface is reached. The critical point (i.e. the point of abrupt increase) is consistent with the demarcation point between valid and invalid data on the D_o - x curve in Fig. 5(a), but it can be picked up more easily on the $\partial D_o / \partial x$ - x curve. For the case with a crack, a similar approach to determine the range of valid data can be adopted. Curves of $\partial D_{eq} / \partial x$ vs x at different times for diffusion through a crack are shown in Fig. 6. The derivative of D_{eq} should approach zero with increasing distance x , but an abrupt increase can be observed due to errors in the numerical results. The critical distance (for a particular time) can again be picked up on the curve of $\partial D_{eq} / \partial x$ vs x .

A second source of error is arising from reflection effect of the bottom boundary of the finite element model. This effect becomes significant for high crack diffusion coefficient D_{cr} and large crack width w . To examine this effect, results obtained from our standard finite element model with depth of 200mm is compared to that from a model of 400mm depth for the same values of D_{cr} , D_o , and w . Results up to a distance of 200mm are shown in Fig. 7. $\partial D_{eq} / \partial x$ vs x curves for the 400mm case (broken lines) show an expected decreasing trend as there is little effect from the far away boundary. For the 200mm case (solid lines), the reflection effect of bottom boundary causes the derivative of D_{eq} to increase. The longer the diffusion age, the higher is the concentration

near the bottom boundary and hence more significant is the reflection effect. A second critical distance is obtained from the rising part of the curve when distance is 200mm.

For a given combination of D_{cr} , D_o , w , the two critical distances described above can be obtained at a given time. The smaller of these two distances is then plotted against time, as illustrated in Fig. 8 to identify the range of valid data. For instance, at a distance 15 cm from the surface, the valid data should be selected between time t_1 and t_2 in Fig. 8. Before t_1 , the numerical results suffer from significant relative error, while after t_2 , the results are affected by boundary reflection. In the following section, only results in the valid range are used as data for the fitting of K for determining an empirical expression for D_{eq} .

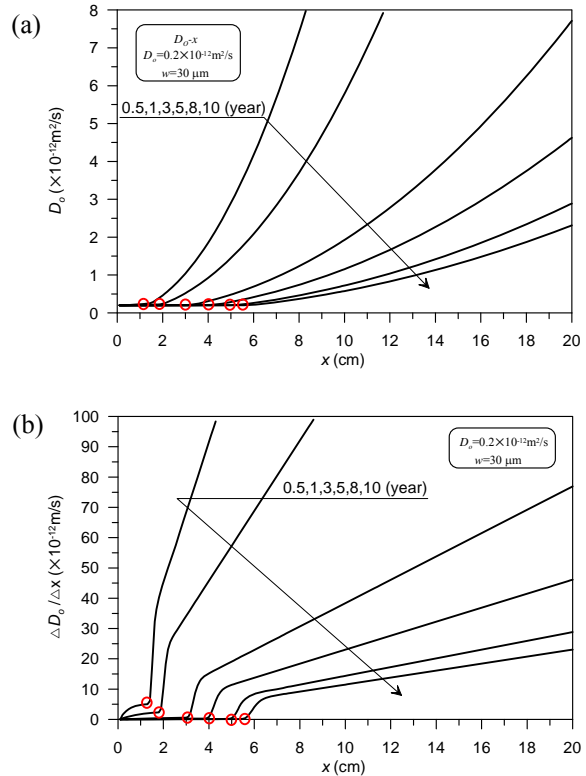


Fig. 5 Validity of D_o calculated by simulation results
 (a) Variations of D_o with x ;
 (b) Variations of derivative of D_o to x with x

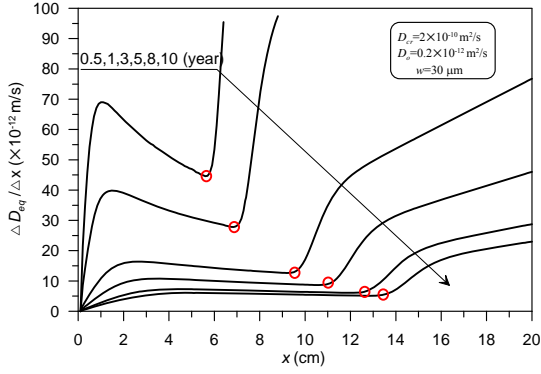


Fig. 6 Curves of $\partial D_{eq}/\partial x$ vs x calculated from simulation results

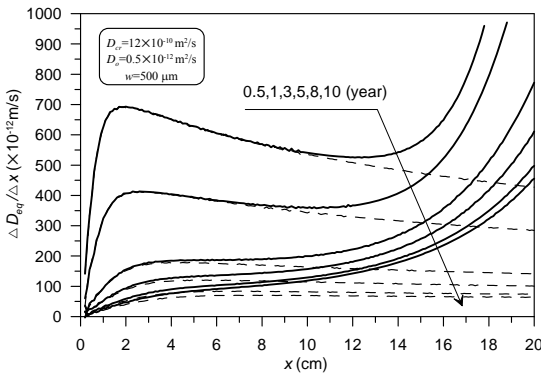


Fig. 7 Effect of bottom boundary reflection on curves of $\partial D_{eq}/\partial x$ vs x

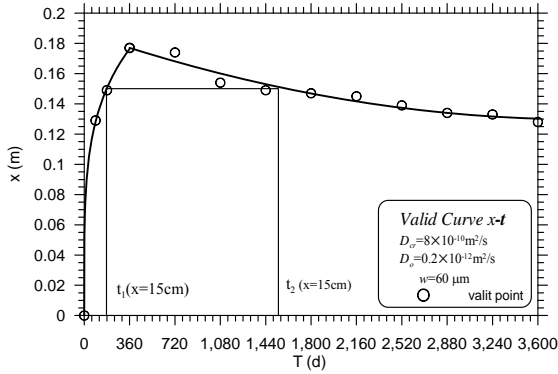


Fig. 8 Range of valid numerical results for fitting

3.3 Modeling and data fitting

As discussed above, the factor K in eqn (4) is governed by D_{cr} (m^2/s), D_o (m^2/s), w (m), x (m) and t (s). To obtain an empirical relation between K and the various parameters, dimensional analysis is first carried out to see how the parameters can be combined. The

dimension of K is unity. Dimensions of parameters of D_{cr} , D_o , x , w , t are M^2T^{-1} , M^2T^{-1} , M , M and T respectively. According to Buckingham π theory [9], the following equation can be obtained:

$$(M^2T^{-1})^{a_1}(M^2T^{-1})^{a_2} M^{a_3}M^{a_4}T^{a_5} = 1 \quad (6)$$

The relations between the indices are then given by:

$$\begin{cases} 2a_1 + 2a_2 + a_3 + a_4 = 0 \\ -a_1 - a_2 + a_5 = 0 \end{cases} \quad (7)$$

Three possible solutions to eqn (7) are $(a_1, a_2, a_3, a_4, a_5) = (0, 1, -2, 0, 1)$, $(1, -1, 0, 0, 0)$ and $(0, 0, 1, -1, 0)$. Based on these three solutions, the independent parameters can be combined as $D_o t/x^2$, D_{cr}/D_o and x/w . With the dimensional analysis method, the number of independent parameters is reduced from 5 to 3. In addition, the relationship in terms of dimensionless parameters can better reflect the physical nature of the diffusion behavior.

From the numerical results, D_{eq} is first calculated and K is obtained from eqn(4). We then attempt to relate K to $D_o t/x^2$ and the following function is found to provide a very good fit.

$$K = \left(\frac{D_{cr}}{D_o} - 1 \right) \frac{k \left(\frac{D_o t}{x^2} \right)^b}{1 + k \left(\frac{D_o t}{x^2} \right)^b} \quad (8)$$

The first term in eqn (8) indicates that when D_{cr} is similar to D_o , K is very small, so D_{eq} is similar to D_{cr} (or D_o). In other words, the crack has little effect on the diffusion process.

Substituting eqn (8) into eqn (4), D_{eq} can be expressed as

$$D_{eq} = \frac{D_{cr} + D_o k \left(\frac{D_o t}{x^2} \right)^b}{1 + k \left(\frac{D_o t}{x^2} \right)^b} \quad (9)$$

The parameters k and b are then expressed as functions of D_{cr}/D_o and x/w , and the following best-fitted expressions are found.

$$b = \frac{\left(\frac{D_{cr}}{D_o}\right)^{0.201}}{0.107 \cdot \left(\frac{D_{cr}}{D_o}\right)^{0.484} + 5.973 \cdot \left(\frac{x}{w}\right)^{-0.109}} \quad (10)$$

$$k = \frac{\left(\frac{x}{w}\right)^{0.073}}{0.390 \cdot \left(\frac{D_{cr}}{D_o}\right)^{-0.0388} - 3.024 \times 10^{-8} \cdot \left(\frac{x}{w}\right)^{1.755}} \quad (11)$$

For all combinations of $D_o t/x^2$, D_{cr}/D_o and x/w used in the finite element analysis, b and k are calculated from eqn (10) and (11), and D_{eq} obtained from eqn(9). To further illustrate the applicability of the empirical expressions, the calculated D_{eq} is substituted into eqn (5) to obtain chloride concentration along the crack under various situations. The results are then compared directly to those from the finite element analysis. Fig.9 (a) shows the variation of chloride concentration with distance from the surface at different times, while Fig.9 (b) shows the variation of chloride concentration with time for different locations along the crack. It is clear from both figures that results from empirical equations (continuous line) are very close to the finite element results (open dots).

As shown in Fig.9 (c), for cases with high crack diffusion coefficient D_{cr} and large crack width w , the chloride concentrations from the empirical model are lower than numerical results at locations far away from boundary with constant chloride concentration. This is caused by the reflection effect of the bottom boundary in the numerical simulations. In the empirical fitting, only data without the reflection effect is selected, so the predictions from the empirical expression should be free of boundary reflection effects and more accurate.

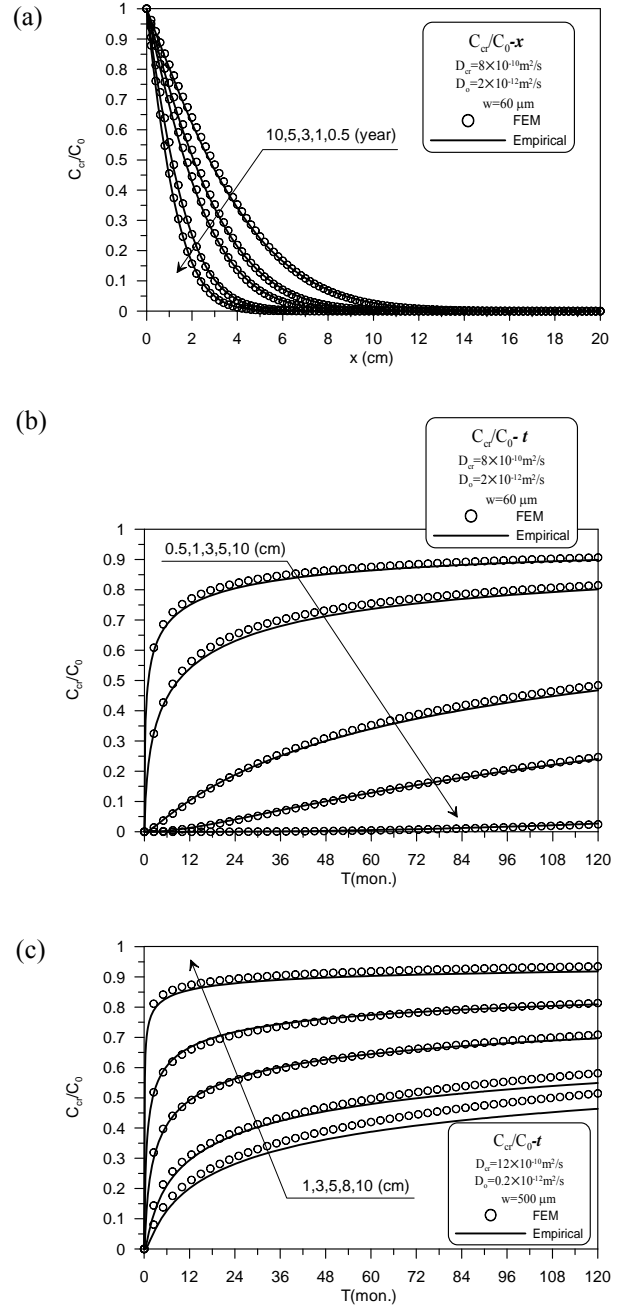


Fig.9 Comparison of chloride concentration from empirical model(continuous line) with finite element analysis (discrete points)
 (a) Chloride concentration along the crack at different times; (b) and (c) Chloride concentration in the crack at different locations vs time

3.4 Time to steel corrosion initiation

As chloride at the steel surface reaches a critical concentration, corrosion starts to occur. The determination of corrosion initiation time

is important in the durability assessment of reinforced concrete structure. Knowing the critical chloride concentration C_{ini} and the surface concentration C_o , eqn (5) can again be employed to obtain the time for C_{ini} to be reached at a particular distance x from the surface (so steel with such a cover will start to rust), or the depth of penetration of the corrosion front (which is the distance from surface where C_{ini} is just reached) at a given time. In the calculation, D_{eq} in eqn (5) are obtained from eqns (9) to (11). Due to the complex form of the empirical equations, eqn (5) cannot be transformed to an explicit analytical form. It is therefore necessary to solve it implicitly through numerical iteration.

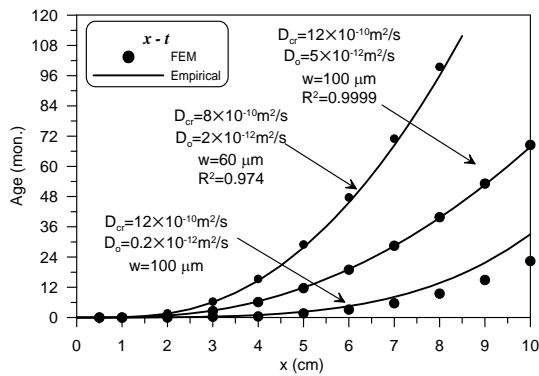


Fig.10 Time to corrosion initiation for various distances from the surface

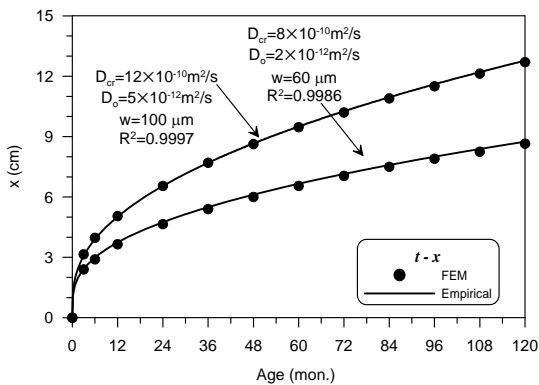


Fig.11 Penetration depth of corrosion front at different times

Fig.10 and Fig.11 show respectively the calculated results for corrosion initiation time at various distances and depth of penetration front at different times. In these calculations, C_{ini}/C_o is taken to be 5%. In both figures, the continuous line represents the result obtained from the empirical model and the dots are finite element results. The good general agreement between the two can again be observed. For the case with $D_{cr}=12 \times 10^{-10} \text{ m}^2/\text{s}$, $D_o=0.2 \times 10^{-12} \text{ m}^2/\text{s}$ and $w=100 \mu\text{m}$ in Fig.11, the predicted corrosion initiation time obtained from the empirical model is higher than that from the finite element analysis at locations far away from surface ($x > 6 \text{ cm}$). This is again due to the reflection effect at the bottom of the finite element mesh which increases the chloride concentration and hence reduces the time for critical chloride concentration to be reached. According to the results in Fig.10, the corrosion initiation time can increase significantly with distance from the surface. This implies a thicker cover is still effective in delaying steel rusting even when the concrete structure exhibits surface cracks.

4 CONCLUSION

For cracked concrete structures exposed to chloride environment, chloride diffusivity through the crack (D_{cr}) is higher than that through the concrete matrix (D_o). As a result, steel corrosion in the cracked member will occur at an earlier time. The analysis of chloride penetration through the crack is a complicated problem as diffusion along the crack is coupled with diffusion perpendicular to the crack resulted from the lateral concentration gradient between the crack and the surrounding matrix. To obtain a good understanding of the diffusion process, finite element analysis is first carried out to obtain the chloride concentration distribution at different times for concrete with different D_o , D_{cr} and crack width (w). Then, after a sufficiently large amount of numerical

data are produced from the simulation, an equivalent diffusion coefficient D_{eq} is derived from empirical fitting, assuming the diffusion to be one-dimensional in nature. D_{eq} obtained in this manner is a function of D_o , w , D_{cr} as well as time and distance from the surface. According to dimensional analysis, D_{eq} can be expressed in terms of three dimensionless parameters. Using the empirically determined D_{eq} , predicted chloride profile, corrosion initiation time and penetration of corrosion front are all in good agreement with finite element results. The approach developed in the present study therefore provides a simple but accurate means for the analysis of chloride diffusion in cracked concrete members.

REFERENCES

- [1] Andrade, C. Calculation of Chloride Diffusion-Coefficients in Concrete from Ionic Migration Measurements. *Cement and Concrete Research*, 1993, 23(3): 724-742.
- [2] Luping Tang, Lars-Olof Nilsson. Rapid Determination of the Chloride Diffusivity in Concrete by Applying an Electric Field. *Materials Journal*, 1993, 89(1): 49-53.
- [3] Arvind K. Suryavanshi, R. Narayan Swamy, George E. Cardew. Estimation of Diffusion Coefficients for Chloride Ion Penetration into Structural Concrete. *Materials Journal*, 2002, 99(5): 441-449.
- [4] Aldea, C.-M., Shah, S.P. and Karr, A. Effect of Cracking on Water and Chloride Permeability of Concrete, *ASCE Journal of Materials in Civil Engineering*, 1999, 11(3), 181-187.
- [5] B. Gérard, J. Marchand, Influence of cracking on the diffusion properties of cement-based materials, Part I: influence of continuous cracks on the steady-state regime, *Cement and Concrete Research*, 2000, 30(1): 37-43.
- [6] Olga, G.R. and Hooton, R.D. Influence of Cracks on Chloride Ingress into Concrete, *ACI Materials Journal*, 2003, 100(2), 120-126.
- [7] Djerbi, A., Bonnet, S., Khelidj, A. and Baroghel-bouny, V. Influence of Traversing Crack on Chloride Diffusion into Concrete, *Cement and Concrete Research*, 2008, 38(6), 877-883.
- [8] Chongshi Wu. *Methods of Mathematical Physics*. Peking University Press, 2011, 181-183.(in chinese)
- [9] Frank R. Giordano, Maurice D. Weir and Willian P. Fox. *A first course in mathematical modeling (third edition)*, China Machine Press, 2003, 304-307.